

## Article

# Modeling of Combined Lead Fast Reactor and Concentrating Solar Power Supercritical Carbon Dioxide Cycles to Demonstrate Feasibility, Efficiency Gains, and Cost Reductions

Brian White <sup>1</sup>, Michael Wagner <sup>1</sup>, Ty Neises <sup>3</sup>, Cory Stansbury <sup>4</sup>, and Ben Lindley <sup>2\*</sup>

<sup>1</sup> Department of Mechanical Engineering, University of Wisconsin - Madison, 1415 University Drive, Madison, WI 53706, United States; dept@me.engr.wisc.edu

<sup>2</sup> Department of Engineering Physics, University of Wisconsin - Madison, 1500 Engineering Drive, Madison, WI 53706, United States; EMAIL

<sup>3</sup> National Renewable Energy Laboratory, Thermal Systems Group, 15013 Denver West Parkway, Golden, CO 80401, United States; EMAIL

<sup>4</sup> Westinghouse Electric Company, Lead Fast Reactor Systems Development, ADDRESS United States; EMAIL

\* Correspondence: lindely2@wisc.edu (B.L.); Tel.: +1-608-265-2001 (B.L.)

**Citation:** White, B.; Lindley, B.; Wagner, M. Modeling of Combined Lead Fast Reactor and Concentrating Solar Power Supercritical Carbon Dioxide Cycles to Demonstrate Feasibility, Efficiency Gains, and Cost Reductions. *Sustainability* **2021**, *1*, 0. <https://doi.org/>

Received:  
Accepted:  
Published:

**Publisher's Note:** MDPI stays neutral with regard to jurisdictional claims in published maps and institutional affiliations.

**Copyright:** © 2021 by the authors. Submitted to *Sustainability* for possible open access publication under the terms and conditions of the Creative Commons Attribution (CC BY) license (<https://creativecommons.org/licenses/by/4.0/>).

**Abstract:** Separate cycles for solar concentrating power and lead fast reactors, which innately have issues with weather, grid demand, and time of day, have potential to benefit when coupled together in a supercritical CO<sub>2</sub> Brayton cycle. Combining these cycles could allow for the lead fast reactor cycle to thermally charge the salt storage in the solar concentrating power cycle during low demand periods and be utilized when grid demand increases. The implementation of the independent cycles into one cycle is modeled to find the preferred location of the lead fast reactor heat exchanger, concentrating solar power heat exchanger, salt charging heat exchanger, turbines, and recuperators within the supercritical CO<sub>2</sub> Brayton cycle. Three cycle configurations have been studied: a two-cycle configuration which uses CSP and LFR heat for dedicated turbocompressors, combined cycle with two high temperature recuperators for both the CSP and LFR, and a combined cycle with CSP and LFR heat sources in parallel. [CONCLUSION]

**Keywords:** Supercritical carbon dioxide Brayton Cycle; Concentrating Solar Power (CSP); Lead Fast Reactor (LFR), Cogeneration, Combined Cycle, Thermal Energy Storage (TES)

## 1. Introduction

## 2. Materials and Methods

### 2.1. Cycle Component Modeling

#### 2.1.1. Counter Flow and Black Box Heat Exchangers

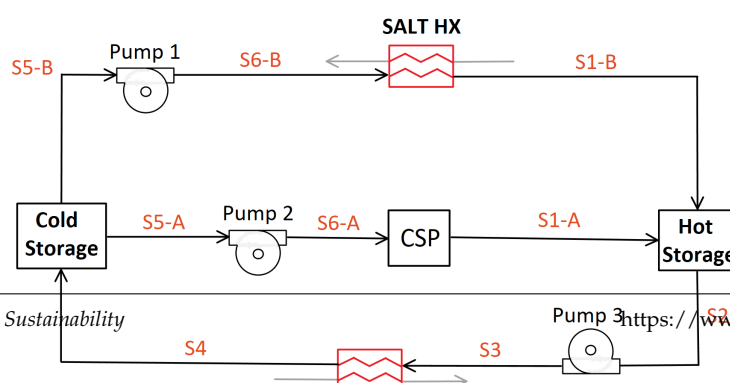
#### 2.1.2. Turbines

#### 2.1.3. Compressors

#### 2.1.4. Lead-Fast Reactor

#### 2.1.5. Concentrating Solar Power Cycle

The CSP cycles modeled in this paper are composed of the hot and cold thermal energy storage, pumps to move the molten salt, and a black box heat input. The diagram for this CSP cycle is seen in Figure 1.



The salt CSP cycle can be either in charging mode or electrical generation mode. When the CSP cycle is in charging mode, excess heat is transferred from the sCO<sub>2</sub> Brayton cycle through the SALT HX. The heated salt is then stored in the hot storage until grid demand increases.

When electrical generation is occurring, the heat input in this cycle is accomplished through a black box energy balance across states S6-A and S1-A with a heat addition of 7.5e8 W from the heliostat field. The hot storage is moved through Pump 3 and transfers heat into the sCO<sub>2</sub> Brayton cycle to be converted into electricity. The cooled salt is stored in cold storage and moved through Pump 2 where the heat addition from the heliostat field is added.

## 2.2. Generalization of Cycle Modeling

The cycles presented are generalized in order to draw a more direct comparison. The generalized parameters include isentropic efficiencies, heat exchanger approach temperatures, pressures, heat input, and pump constants. These values are summarized in Table 1.

**Table 1.** Constant cycle parameters with definition, variable and set value.

Parameter	Variable	Design Point Value
<i>Efficiencies</i>		
Main Compressor	$\eta_{MC}$	0.91 (-)
Re-Compressor	$\eta_{RC}$	0.89 (-)
Turbine	$\eta_T$	0.90 (-)
Pump	$\eta_P$	0.90 (-)
<i>Approach Temperatures</i>		
Low Temperature Recuperator	$\delta_{LTR}$	10 (K)
High Temperature Recuperator	$\delta_{HTR}$	10 (K)
Concentrating Solar Power Heat Exchanger	$\delta_{CSPHX}$	10 (K)
<i>Pressures</i>		
Pressure Ratio	$PR$	3.27 (-)
High Side Pressure	$P_{2A}$	2.88e7 (Pa)
<i>Heat Into System</i>		
Lead-Fast Reactor Heat Transfer	$\dot{Q}_{LFRHX}$	9.5e8 (W)
Concentrating Solar Power Heat Transfer	$\dot{Q}_{CSP}$	7.5e8 (W)
<i>Temperature</i>		
Main Compressor Inlet	$T_{1A}$	313.2 (K)
Lead-Fast Reactor sCO <sub>2</sub> High Temperature	$T_5, T_{2C}, T_{6A}, T_{5C}$	868.2 (K)
<i>Pumps</i>		
Pressure Rise Across Pump	$\Delta_P$	3.726e6 (Pa)
Pump Low Side Pressure	$P_{S5-B}$	3.0e6 (Pa)

The values displayed in Table 1 are representative of LFR and CSP design while being consistent with design parameters given by our industry partner, Westinghouse Electric Corporation.

In addition to generalized parameters, all cycles have identical recompression sides. The recompression side contains a PreCooler, Low Temperature Recuperator, and two compressors; Main Compressor and ReCompressor.

## 2.3. Non-Charging Cycle Configurations

Various cycles are modeled to test their advantages and disadvantages. These cycle models fall into two categories: non-charging and charging. The non-charging category decides the configuration of the cycle with a focus on electricity generation. This includes

the number and location of turbines, recuperators, and heat input to the system by the CSP and LFR. To quantify the effectiveness of the non-charging configurations, a cycle efficiency,  $\eta_{cycle}$ , is defined in Equation 1.

$$\eta_{heatstorage} = \frac{\dot{W}_T - \dot{W}_{MC} - \dot{W}_{RC}}{\dot{Q}_{LFRHX} + \dot{Q}_{CSPHX}}, \quad (1)$$

The numerator in Equation 1 is the Alternator power, or the power produced from the turbines,  $\dot{W}_T$ , minus the required power of the compressors,  $\dot{W}_{MC}$  and  $\dot{W}_{RC}$ . The denominator is the total power input into the system from the LFR,  $\dot{Q}_{LFRHX}$ , and CSP,  $\dot{Q}_{CSPHX}$ .

### 2.3.1. Two-Cycle Configuration: C-LFR-ON and C-CSP-ON

The two-cycle configuration that is tested has independent sCO<sub>2</sub> loops bridged by a salt CSP cycle. This cycle has two sCO<sub>2</sub> Brayton Cycles: C-LFR-ON and C-CSP-ON. Configuration of components for these two cycles is identical with the exception of heat inputs. C-LFR-ON has heat provided from a LFR while C-CSP-ON has heat provided from a CSP. These two cycles individually operate when the focus of plant operation is primarily electricity generation.

The LFR cycle for this two-cycle configuration is labeled as C-LFR-ON and the cycle diagram is illustrated in Figure 2.

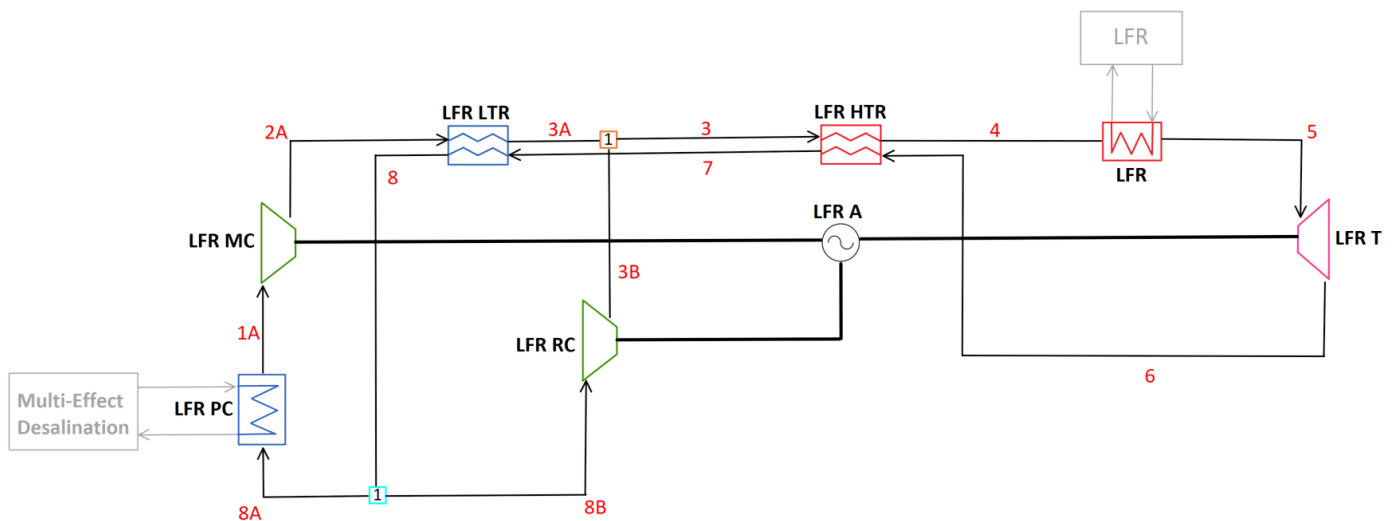
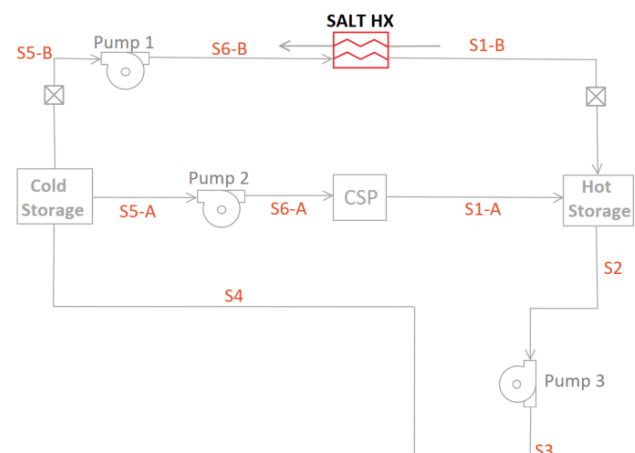


Figure 2. Diagram for C-LFR-ON with focus on electricity generation

Two separate sensitivity studies on the LFR inlet temperature are completed for C-LFR-ON. The unconstrained study is performed by gradually increasing the mass flow to the main compressor while maximizing cycle efficiency. The constrained study is calculated by setting the LFR inlet temperature to the design value of 673.2 K.

The CSP cycle for this two-cycle configuration is labeled C-CSP-ON and the cycle diagram is shown in Figure 3. The diagram has the necessary pumps, TES tanks, and salt heat exchangers to be representative of a reliable salt CSP cycle.



Due to the individual operation while the cycles are generating electricity, C-CSP-ON is not directly impacted by the LFR low end temperatures. Instead, a sensitivity study is done on the temperature of the cold TES. Two temperatures are tested, 663.2 K and 713.2 K, to observe the impact of cold TES temperature on cycle efficiency.

### 2.3.2. C-1HTR1T-ON

One drawback of having a two-cycle design, as seen in the C-LFR-ON and C-CSP-ON, is doubling the number of system components. Combining the two cycles into one would reduce redundancy and complexity. Heat addition from the CSP and LFR in parallel orientation is therefore studied in the C-1HTR1T-ON model. This model studies what impact mixing different temperature flows prior to the turbine has on cycle efficiency. The diagram for this cycle is illustrated in Figure 4.

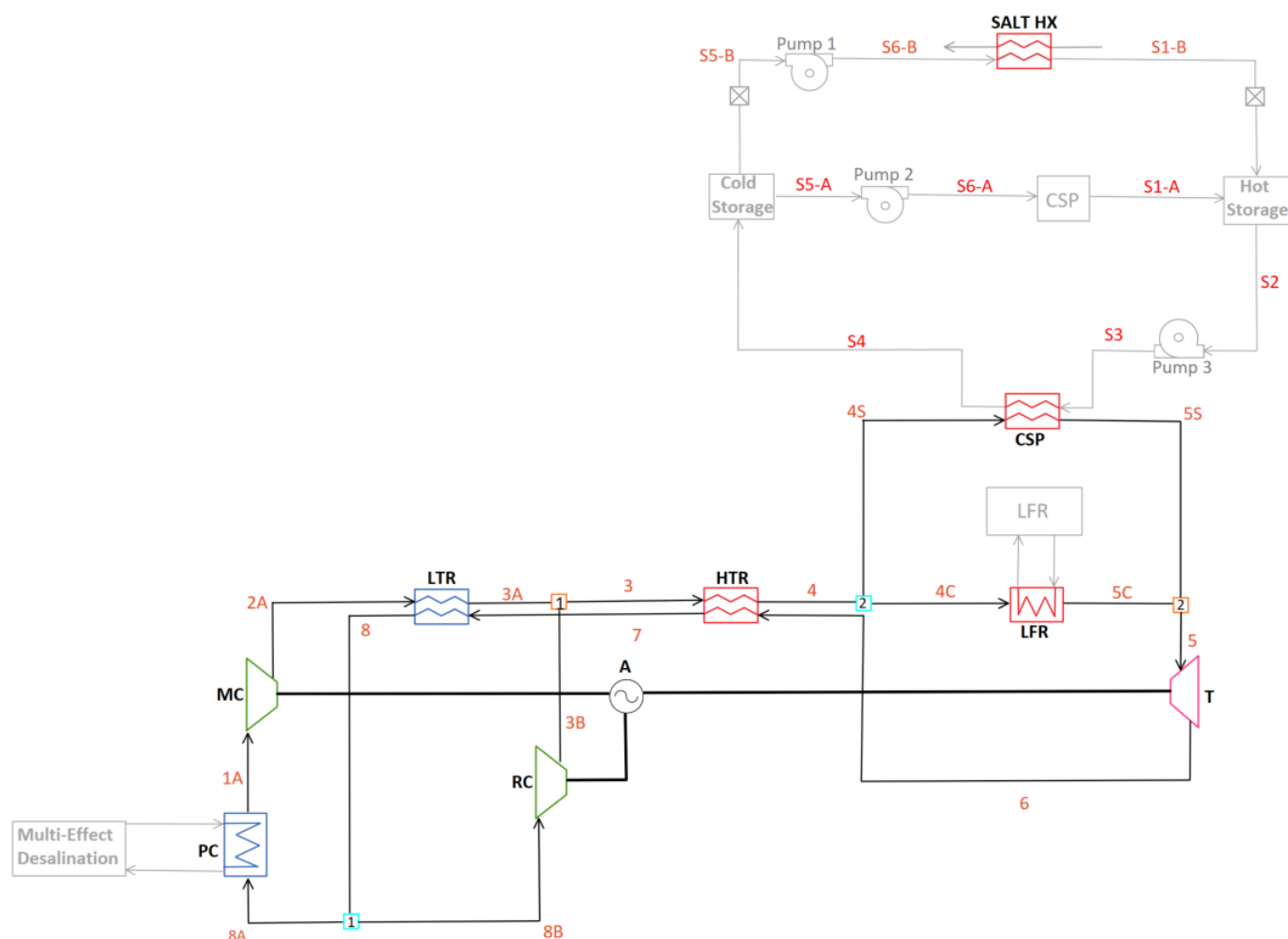


**Figure 4.** Diagram for C-1HTR1T-ON with focus on electricity generation

In this cycle, the LFR and CSP have identical inlet temperatures due to splitting the flow prior to their parallel orientation. Therefore, three sensitivity studies are done on the C-1HTR1T-ON EES model. The initial two studies have the low LFR temperature constrained to the value of 673.2 K with varied cold CSP TES and maximized cycle efficiency. The two tested values for cold CSP TES with constrained LFR low temperature are 683.2 K and 713.2 K. The desired cold CSP TES temperature of 663.2 K is not possible with the constraint on the LFR low temperature. To obtain the desired cold CSP TES temperature, the constraint on the LFR low temperature is removed, dropping the temperature of the LFR inlet to 653.2 K.

### 2.3.3. C-2HTR3T-ON

Mixing two different temperature flows before the turbine in a Brayton cycle has a negative effect on cycle efficiency. To quantify the reduction in cycle efficiency, another cycle with no mixing prior to the turbine is desired. This cycle, C-2HTR3T-ON, can be seen in Figure 5 and has two high temperature recuperators and three turbines. The LFR is powering one turbine, T1, and recuperating heat through a dedicated high temperature recuperator, HTR1. The CSP cycle also contains two separate turbines, T2, while having a dedicated high temperature recuperator, HTR2. After the high temperature recuperators, the two flows are combined and sent to the LTR hot side.

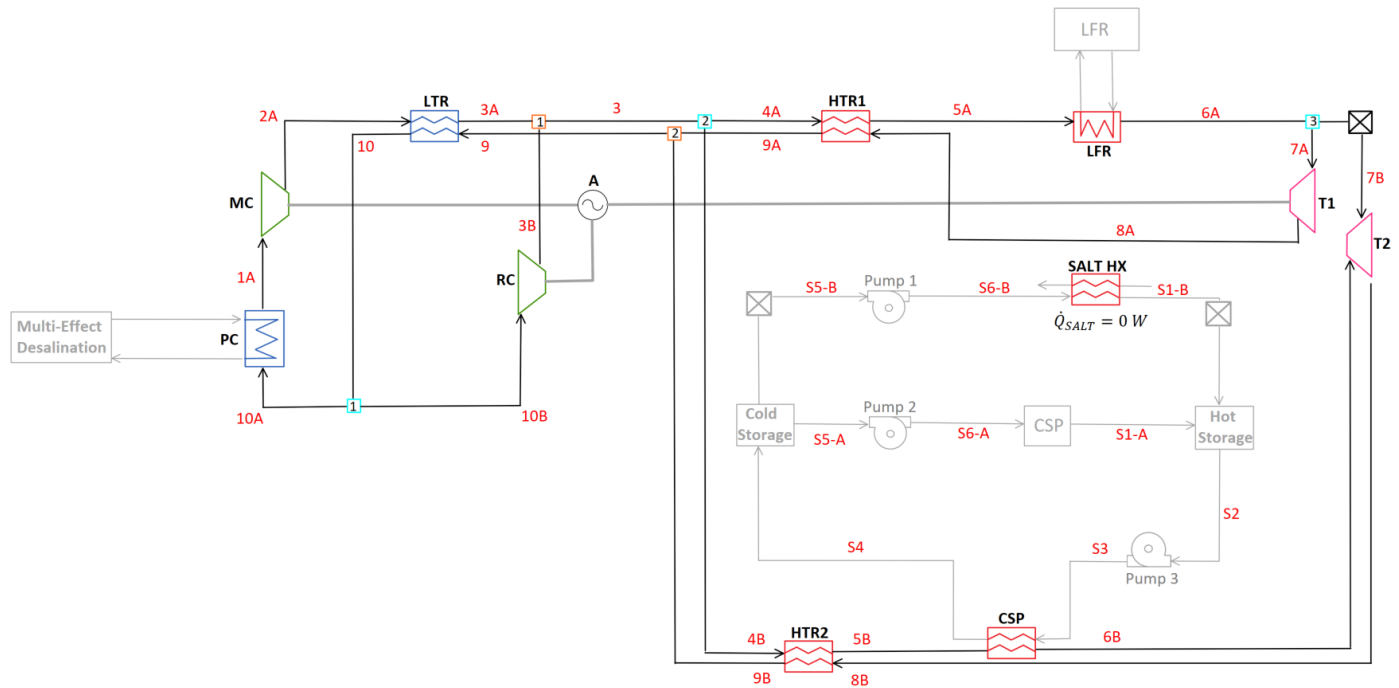


**Figure 5.** Diagram for C-2HTR3T-ON with focus on electricity generation

Three sensitivity studies are done on the C-2HTR3T-ON model. Two with the LFR low temperature constrained and one without this constraint. The two constrained studies had varied cold CSP TES temperature with the lowest temperature of 663.2 K and highest temperature of 713.2 K. The unconstrained low LFR inlet study is calculated at a cold CSP TES temperature of 663.2 K.

### 2.4. Thermal Energy Storage Charging Techniques

Charging cycle configurations focus on an energy storage operating mode. These configurations test the optimal location of LFR heat extraction through the SALT HX. To maximize the available heat for extraction, alternator power is set to zero and turbine power is therefore equal to the compressors' demand. The excess energy from the LFR is thermally stored in the TES for later use when grid demand increases. Comparison of where thermal energy is extracted in the cycle is done by using the same Brayton cycle, C-LFR-ON, and configuring the salt heat exchanger in different locations around the turbine. To quantify the effectiveness of TES charging techniques a heat storage efficiency,  $\eta_{heatstorage}$ , is defined by Equation 2.

$$\eta_{heatstorage} = \frac{\dot{Q}_{SALT}}{\dot{Q}_{LFRHX} + \dot{Q}_{CSPHX}}, \quad (2)$$

Whereas  $\dot{Q}_{SALT}$  is the amount of heat transferred through the SALT HX and the addition of  $\dot{Q}_{LFRHX}$  and  $\dot{Q}_{CSPHX}$  is the total amount of heat input into the system from the LFR and CSP.

#### 2.4.1. C-LFR-PRE

Flow leaving the turbine contains excess thermal energy that is not transformed into electrical energy. This excess thermal energy is stored in the hot CSP TES. The diagram outlining this process is C-LFR-PRE in Fig. 6.

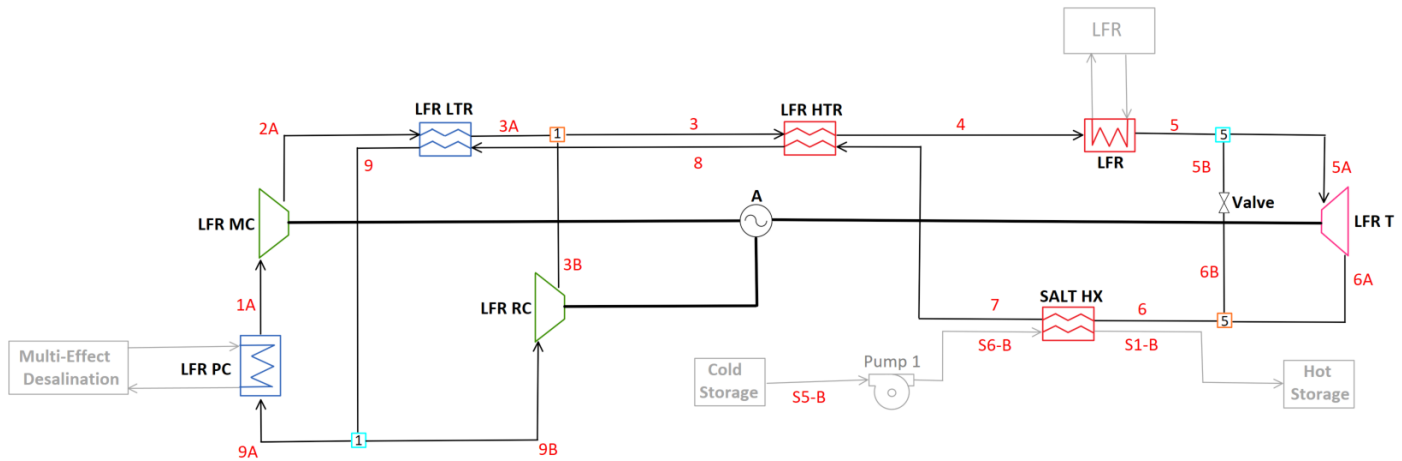


**Figure 6.** Diagram for C-LFR-PRE thermal energy storage charging orientation

Problems arise with this salt charging configuration. The temperature out of the turbine is not high enough to charge the hot CSP TES to the required value of 833.2 K. To raise the temperature, some of the high temperature flow before the turbine is redirected through a valve and combined after the turbine. Combining different temperature flows and reducing the flow through the turbine has a large impact on heat storage efficiency.

#### 2.4.2. C-LFR-POST

Moving the heat extraction prior to the turbine is analyzed in C-LFR-POST. This diagram is seen in Figure 7.

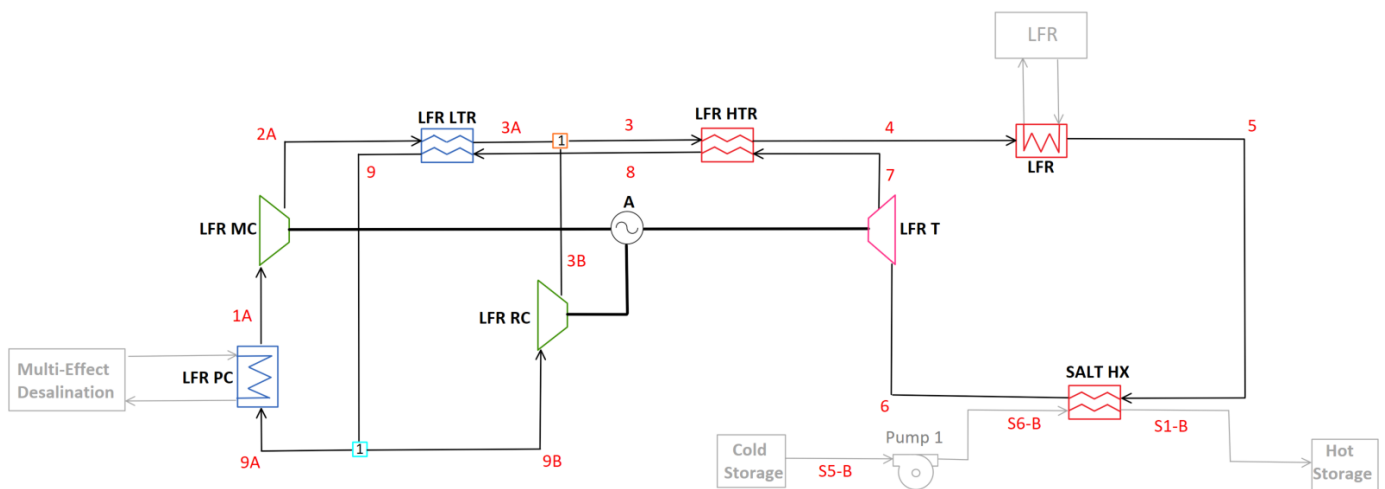


**Figure 7.** Diagram for C-LFR-POST thermal energy storage charging orientation

This TES charging cycle extracts heat before the turbine and therefore would have a large negative effect on the amount of work that the turbine could produce. The

turbine needs to offset the requirements of both compressors and this would require the inlet temperature to be high. The amount of energy that could be extracted before the turbine would be small and therefore the heat storage efficiency would be small. There is no quantitative study done on this diagram because, due to the efficiency losses, it is non-viable.

### 2.4.3. C-LFR-PAR

The requirement of the turbine and CSP hot TES temperature can be accomplished by splitting the flow before the turbine. The flow through the salt heat exchanger in this cycle is therefore separate from the turbine. After the salt heat exchanger a valve is needed to reduce the pressure, this TES charging cycle is C-LFR-PAR shown in Figure 8.

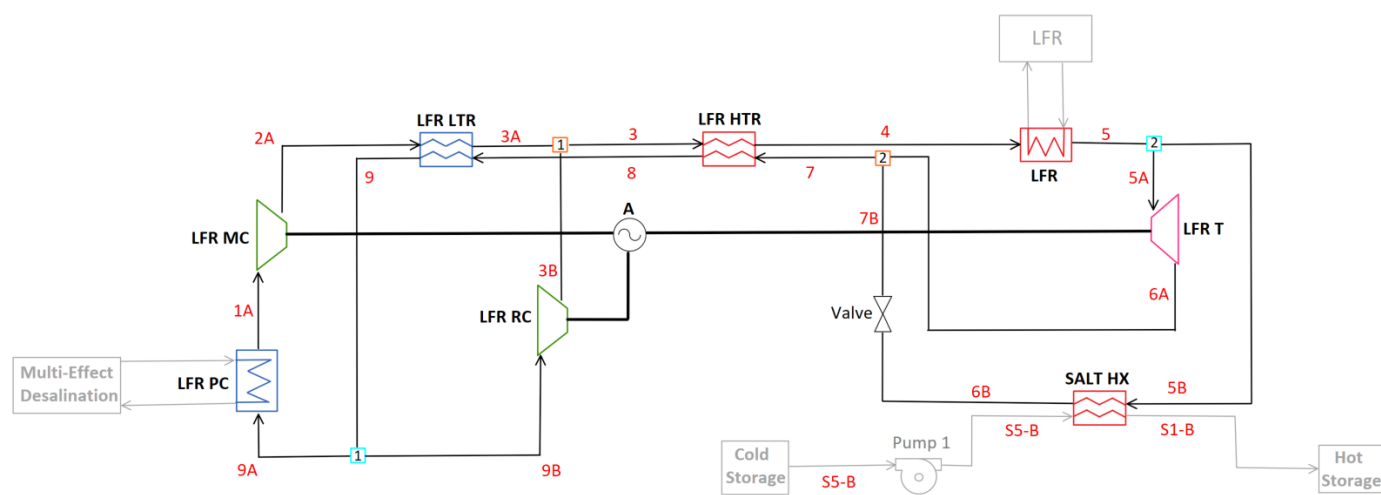


Figure 8. Diagram for C-LFR-PAR thermal energy storage charging orientation

Two sensitivity studies with varying cold CSP TES are desired to see the impact on heat storage efficiency. The TES temperature study is calculated with a low TES temperature of 663.2 K and a high TES temperature of 713.2 K.

### 2.4.4. C-LFR-CIRC

The full diagram for C-LFR-CIRC is shown in Figure 9.

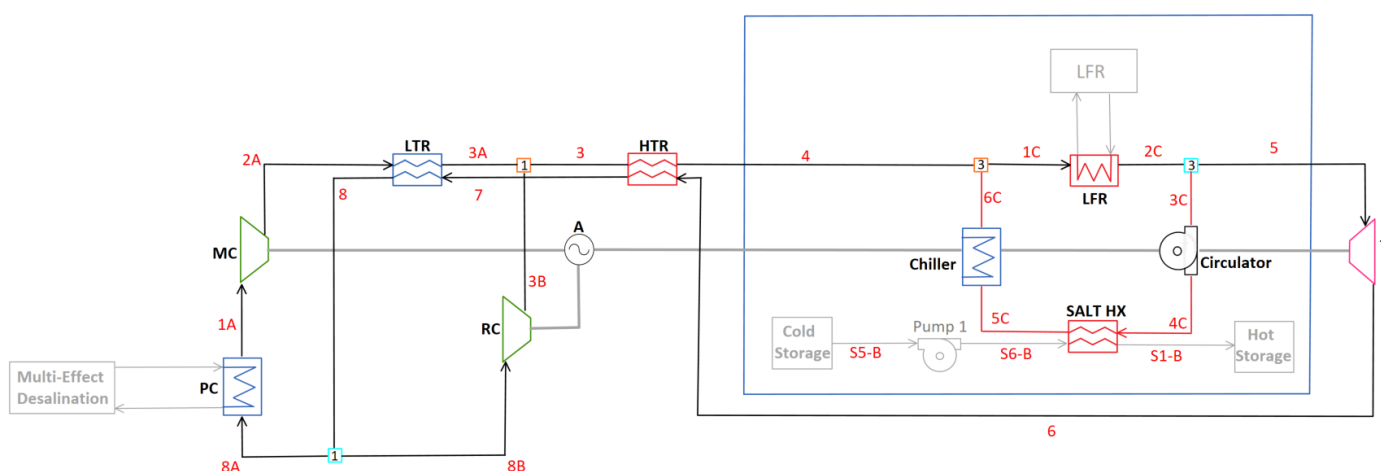
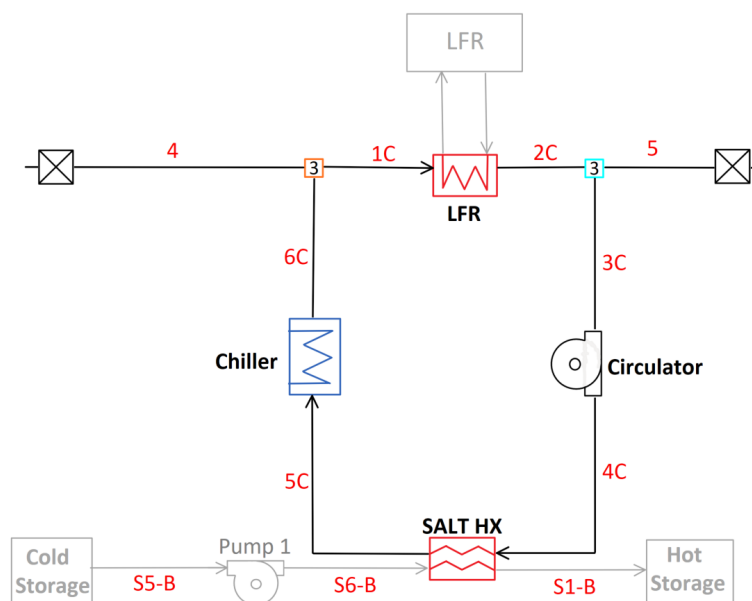


Figure 9. Full diagram for C-LFR-CIRC thermal energy storage charging orientation

149 The charging subsection of this diagram is composed of a circulation cycle that has  
 150 heat inputted through the LFR heat exchanger. This subsection is encircled in blue and  
 151 can be seen in Figure 10.



**Figure 10.** Diagram for C-LFR-CIRC subcycle thermal energy storage charging orientation

152 The flow continues through a circulator which is assumed to have negligible  
 153 pressure rise. A heat exchanger, SALT HX, extracts heat from the flow, storing the  
 154 thermal energy in the hot TES for later use. Excess heat that is not extracted is then  
 155 dumped into a reservoir through the chiller to bring the temperature of the flow down  
 156 to LFR cool side operating temperature of 673.2 K. Three different temperatures; 663.2 K,  
 157 683.2 K, and 713.2 K, are compared in a sensitivity study.

### 158 3. Results

#### 159 3.1. Non-Charging Cycle Configurations

##### 160 3.1.1. C-LFR-ON and C-CSP-ON

161 Modeling the C-LFR-ON cycle in EES yielded the results in Table 2.



**Table 2.** Calculated system parameters for non-charging C-LFR-ON cycle configuration with constrained (C) and unconstrained (U) Lead-Fast Reactor low-end temperature.

Definition	Variable	U	C
LFR Inlet Temperature (K)	$T_4$	Data	Data
Cycle Efficiency (%)	$\eta_{cycle}$	Data	Data
Alternator Power (W)	$\dot{W}_A$	Data	Data
PC Heat Transfer	$\dot{Q}_{PC}$	Data	Data
MC Power (W)	$\dot{W}_{MC}$	Data	Data
RC Power (W)	$\dot{W}_{RC}$	Data	Data
Turbine Power (W)	$\dot{W}_T$	Data	Data
MC Mass Flow Fraction (-)	$y_1$	Data	Data
LTR UA Value (W/K)	$UA_{LTR}$	Data	Data
LTR Capacitance Ratio (-)	$CR_{LTR}$	Data	Data
LTR Heat Transfer Rate (W)	$\dot{Q}_{LTR}$	Data	Data
LTR Effectiveness (-)	$\varepsilon_{LTR}$	Data	Data
HTR UA Value (W/K)	$UA_{HTR}$	Data	Data
HTR Capacitance Ratio (-)	$CR_{HTR}$	Data	Data
HTR Heat Transfer Rate (W)	$\dot{Q}_{HTR}$	Data	Data
HTR Effectiveness (-)	$\varepsilon_{HTR}$	Data	Data

## Discussion of Results

The EES model outputs for C-CSP-ON are listed in Table 3.

**Table 3.** Calculated system parameters for non-charging C-CSP-ON cycle configuration with varied TES cold temperature.

Definition	Variable		
Cold TES Temperature (K)	$T_{CS}$	Data	Data
Cycle Efficiency (%)	$\eta_{cycle}$	Data	Data
Alternator Power (W)	$\dot{W}_A$	Data	Data
PC Heat Transfer	$\dot{Q}_{PC}$	Data	Data
MC Power (W)	$\dot{W}_{MC}$	Data	Data
RC Power (W)	$\dot{W}_{RC}$	Data	Data
Turbine Power (W)	$\dot{W}_T$	Data	Data
MC Mass Flow Fraction (-)	$y_1$	Data	Data
LTR UA Value (W/K)	$UA_{LTR}$	Data	Data
LTR Capacitance Ratio (-)	$CR_{LTR}$	Data	Data
LTR Heat Transfer Rate (W)	$\dot{Q}_{LTR}$	Data	Data
LTR Effectiveness (-)	$\varepsilon_{LTR}$	Data	Data
HTR UA Value (W/K)	$UA_{HTR}$	Data	Data
HTR Capacitance Ratio (-)	$CR_{HTR}$	Data	Data
HTR Heat Transfer Rate (W)	$\dot{Q}_{HTR}$	Data	Data
HTR Effectiveness (-)	$\varepsilon_{HTR}$	Data	Data
CSPHX UA Value (W/K)	$UA_{CSPHX}$	Data	Data
CSPHX Capacitance Ratio (-)	$CR_{CSPHX}$	Data	Data
CSPHX Heat Transfer Rate (W)	$\dot{Q}_{CSPHX}$	Data	Data
CSPHX Effectiveness (-)	$\varepsilon_{CSPHX}$	Data	Data

## Discussion of Results

### 3.1.2. C-1HTR1T-ON

These values are displayed in Table 4.

**Table 4.** Calculated system parameters for non-charging C-1HTR1T-ON cycle configuration with constrained (C) and unconstrained (U) Lead-Fast Reactor low-end temperature. Temperature of TES cold temperature is also varied.

Definition	Variable	C-1HTR1T-ON		
		U	C	C
Cold TES Temperature (K)	$T_{CS}$	Data	Data	Data
LFR Inlet Temperature (K)	$T_{4C}$	Data	Data	Data
Cycle Efficiency (%)	$\eta_{cycle}$	Data	Data	Data
Alternator Power (W)	$\dot{W}_A$	Data	Data	Data
PC Heat Transfer	$\dot{Q}_{PC}$	Data	Data	Data
MC Power (W)	$\dot{W}_{MC}$	Data	Data	Data
RC Power (W)	$\dot{W}_{RC}$	Data	Data	Data
Turbine Power (W)	$\dot{W}_T$	Data	Data	Data
MC Mass Flow Fraction (-)	$y_1$	Data	Data	Data
LFR Mass Flow Fraction (-)	$y_2$	Data	Data	Data
LTR UA Value (W/K)	$UA_{LTR}$	Data	Data	Data
LTR Capacitance Ratio (-)	$CR_{LTR}$	Data	Data	Data
LTR Heat Transfer Rate (W)	$\dot{Q}_{LTR}$	Data	Data	Data
LTR Effectiveness (-)	$\varepsilon_{LTR}$	Data	Data	Data
HTR UA Value (W/K)	$UA_{HTR}$	Data	Data	Data
HTR Capacitance Ratio (-)	$CR_{HTR}$	Data	Data	Data
HTR Heat Transfer Rate (W)	$\dot{Q}_{HTR}$	Data	Data	Data
HTR Effectiveness (-)	$\varepsilon_{HTR}$	Data	Data	Data
CSPHX UA Value (W/K)	$UA_{CSPHX}$	Data	Data	Data
CSPHX Capacitance Ratio (-)	$CR_{CSPHX}$	Data	Data	Data
CSPHX Heat Transfer Rate (W)	$\dot{Q}_{CSPHX}$	Data	Data	Data
CSPHX Effectiveness (-)	$\varepsilon_{CSPHX}$	Data	Data	Data

## Discussion of Results

### 3.1.3. C-2HTR3T-ON

The calculated values from these studies are displayed in Table 5.

**Table 5.** Calculated system parameters for non-charging C-2HTR3T-ON cycle configuration with constrained (C) and unconstrained (U) Lead-Fast Reactor low-end temperature.

Definition	Variable	C-2HTR3T-ON		
		U	C	C
Cold TES Temperature (K)	$T_{CS}$	Data	Data	Data
LFR Inlet Temperature (K)	$T_{5A}$	Data	Data	Data
Cycle Efficiency (%)	$\eta_{cycle}$	Data	Data	Data
Alternator Power (W)	$\dot{W}_A$	Data	Data	Data
PC Heat Transfer	$\dot{Q}_{PC}$	Data	Data	Data
MC Power (W)	$\dot{W}_{MC}$	Data	Data	Data
RC Power (W)	$\dot{W}_{RC}$	Data	Data	Data
T1 Power (W)	$\dot{W}_{T1}$	Data	Data	Data
T2 Power (W)	$\dot{W}_{T2}$	Data	Data	Data
MC Mass Flow Fraction (-)	$y_1$	Data	Data	Data
LFR Mass Flow Fraction (-)	$y_2$	Data	Data	Data
LTR UA Value (W/K)	$UA_{LTR}$	Data	Data	Data
LTR Capacitance Ratio (-)	$CR_{LTR}$	Data	Data	Data
LTR Heat Transfer Rate (W)	$\dot{Q}_{LTR}$	Data	Data	Data
LTR Effectiveness (-)	$\varepsilon_{LTR}$	Data	Data	Data
HTR1 UA Value (W/K)	$UA_{HTR1}$	Data	Data	Data
HTR1 Capacitance Ratio (-)	$CR_{HTR1}$	Data	Data	Data
HTR1 Heat Transfer Rate (W)	$\dot{Q}_{HTR1}$	Data	Data	Data
HTR1 Effectiveness (-)	$\varepsilon_{HTR1}$	Data	Data	Data
HTR2 UA Value (W/K)	$UA_{HTR2}$	Data	Data	Data
HTR2 Capacitance Ratio (-)	$CR_{HTR2}$	Data	Data	Data
HTR2 Heat Transfer Rate (W)	$\dot{Q}_{HTR2}$	Data	Data	Data
HTR2 Effectiveness (-)	$\varepsilon_{HTR2}$	Data	Data	Data
CSPHX UA Value (W/K)	$UA_{CSPHX}$	Data	Data	Data
CSPHX Capacitance Ratio (-)	$CR_{CSPHX}$	Data	Data	Data
CSPHX Heat Transfer Rate (W)	$\dot{Q}_{CSPHX}$	Data	Data	Data
CSPHX Effectiveness (-)	$\varepsilon_{CSPHX}$	Data	Data	Data

## Discussion of Results

### 3.2. Thermal Energy Storage Charging Techniques

#### 3.2.1. C-LFR-PRE

The calculations from this TES charging technique are shown in Table 6.

**Table 6.** Calculated system parameters for salt charging C-LFR-PRE cycle configuration with TES cold storage set to 663.2 K.

Definition	Variable	C-LFR-PRE C
Cold TES Temperature (K)	$T_{CS}$	Data
LFR Inlet Temperature (K)	$T_4$	Data
Heat Storage Efficiency (%)	$\eta_{heatstorage}$	Data
Alternator Power (W)	$\dot{W}_A$	Data
PC Heat Transfer	$\dot{Q}_{PC}$	Data
MC Power (W)	$\dot{W}_{MC}$	Data
RC Power (W)	$\dot{W}_{RC}$	Data
Turbine Power (W)	$\dot{W}_T$	Data
MC Mass Flow Fraction (-)	$y_1$	Data
Valve Mass Flow Fraction (-)	$y_5$	Data
LTR UA Value (W/K)	$UA_{LTR}$	Data
LTR Capacitance Ratio (-)	$CR_{LTR}$	Data
LTR Heat Transfer Rate (W)	$\dot{Q}_{LTR}$	Data
LTR Effectiveness (-)	$\varepsilon_{LTR}$	Data
HTR UA Value (W/K)	$UA_{HTR}$	Data
HTR Capacitance Ratio (-)	$CR_{HTR}$	Data
HTR Heat Transfer Rate (W)	$\dot{Q}_{HTR}$	Data
HTR Effectiveness (-)	$\varepsilon_{HTR}$	Data
CSPHX UA Value (W/K)	$UA_{CSPHX}$	Data
CSPHX Capacitance Ratio (-)	$CR_{CSPHX}$	Data
CSPHX Heat Transfer Rate (W)	$\dot{Q}_{CSPHX}$	Data
CSPHX Effectiveness (-)	$\varepsilon_{CSPHX}$	Data

## Discussion of Results

### 3.2.2. C-LFR-POST

### 3.2.3. C-LFR-PAR

The results from this study are displayed in Table 7.

**Table 7.** Calculated system parameters for salt charging C-LFR-PAR cycle configuration with TES cold storage varied and LFR low temperature set to 673.2 K.

Definition	Variable	C-2HTR3T-ON	
		C	C
Cold TES Temperature (K)	$T_{CS}$	Data	Data
LFR Inlet Temperature (K)	$T_4$	Data	Data
Heat Storage Efficiency (%)	$\eta_{heatstorage}$	Data	Data
Alternator Power (W)	$\dot{W}_A$	Data	Data
PC Heat Transfer	$\dot{Q}_{PC}$	Data	Data
MC Power (W)	$\dot{W}_{MC}$	Data	Data
RC Power (W)	$\dot{W}_{RC}$	Data	Data
Turbine Power (W)	$\dot{W}_T$	Data	Data
MC Mass Flow Fraction (-)	$y_1$	Data	Data
SALT HX Mass Flow Fraction (-)	$y_2$	Data	Data
LTR UA Value (W/K)	$UA_{LTR}$	Data	Data
LTR Capacitance Ratio (-)	$CR_{LTR}$	Data	Data
LTR Heat Transfer Rate (W)	$\dot{Q}_{LTR}$	Data	Data
LTR Effectiveness (-)	$\varepsilon_{LTR}$	Data	Data
HTR UA Value (W/K)	$UA_{HTR}$	Data	Data
HTR Capacitance Ratio (-)	$CR_{HTR}$	Data	Data
HTR Heat Transfer Rate (W)	$\dot{Q}_{HTR}$	Data	Data
HTR Effectiveness (-)	$\varepsilon_{HTR}$	Data	Data
CSPHX UA Value (W/K)	$UA_{CSPHX}$	Data	Data
CSPHX Capacitance Ratio (-)	$CR_{CSPHX}$	Data	Data
CSPHX Heat Transfer Rate (W)	$\dot{Q}_{CSPHX}$	Data	Data
CSPHX Effectiveness (-)	$\varepsilon_{CSPHX}$	Data	Data
CSPHX Approach Temperature (K)	$\delta_{CSPHX}$	Data	Data

178 Changing the temperature of the cold CSP TES had little effect on the heat storage  
 179 efficiency. The CSP salt mass flow rate and approach temperature of the SALT HX  
 180 would adjust according to the temperature difference in the TES and keep the efficiency  
 181 constant.

#### 182 3.2.4. C-LFR-CIRC

183 Table 8 to show cold thermal energy storage's affect on heat storage efficiency.

**Table 8.** Calculated system parameters for charging C-LFR-CIRC subcycle configuration with constrained Lead-Fast Reactor low-end temperature.

Definition	Variable	C-LFR-CIRC		
Cold TES Temperature (K)	$T_{CS}$	Data	Data	Data
LFR Inlet Temperature (K)	$T_{1C}$	Data	Data	Data
Heat Storage Efficiency (%)	$\eta_{heatstorage}$	Data	Data	Data
Chiller Heat Transfer (W)	$\dot{Q}_{chill}$	Data	Data	Data
CSPHX UA Value (W/K)	$UA_{CSPHX}$	Data	Data	Data
CSPHX Capacitance Ratio (-)	$CR_{CSPHX}$	Data	Data	Data
CSPHX Heat Transfer Rate (W)	$\dot{Q}_{CSPHX}$	Data	Data	Data
CSPHX Effectiveness (-)	$\varepsilon_{CSPHX}$	Data	Data	Data

#### 184 4. Discussion

185 Authors should discuss the results and how they can be interpreted from the  
 186 perspective of previous studies and of the working hypotheses. The findings and their  
 187 implications should be discussed in the broadest context possible. Future research  
 188 directions may also be highlighted.

## 5. Conclusions

This section is not mandatory, but can be added to the manuscript if the discussion is unusually long or complex.

## 6. how to use

### 6.1. Subsection

Citing a journal paper [1]. Now citing a book reference [2] or other reference types [3]. [4]

#### 6.1.1. Subsubsection

Bulleted lists look like this:

- First bullet;
- Second bullet;
- Third bullet.

Numbered lists can be added as follows:

1. First item;
2. Second item;
3. Third item.

The text continues here.

### 6.2. Figures, Tables and Schemes

All figures and tables should be cited in the main text as Figure 11, Table 9, etc.



**Figure 11.** This is a figure. Schemes follow the same formatting. If there are multiple panels, they should be listed as: (a) Description of what is contained in the first panel. (b) Description of what is contained in the second panel. Figures should be placed in the main text near to the first time they are cited. A caption on a single line should be centered.

**Table 9.** This is a table caption. Tables should be placed in the main text near to the first time they are cited.

Title 1	Title 2	Title 3
Entry 1	Data	Data
Entry 2	Data	Data

Text.

Text.

### 210 6.3. Formatting of Mathematical Components

This is the example 1 of equation:

$$a = 1, \quad (3)$$

211 the text following an equation need not be a new paragraph. Please punctuate  
212 equations as regular text.

213 This is the example 2 of equation:

$$\begin{aligned} a &= b + c + d + e + f + g + h + i + j + k + l \\ &+ m + n + o + p + q + r + s + t + u + v + w + x + y + z \end{aligned} \quad (4)$$

214 Please punctuate equations as regular text. Theorem-type environments (including  
215 propositions, lemmas, corollaries etc.) can be formatted as follows:

216 **Theorem 1.** *Example text of a theorem.*

217 The text continues here. Proofs must be formatted as follows:

218 **Proof of Theorem 1.** Text of the proof. Note that the phrase “of Theorem 1” is optional  
219 if it is clear which theorem is being referred to.  $\square$

220 The text continues here.

**Author Contributions:** For research articles with several authors, a short paragraph specifying their individual contributions must be provided. The following statements should be used “Conceptualization, X.X. and Y.Y.; methodology, X.X.; software, X.X.; validation, X.X., Y.Y. and Z.Z.; formal analysis, X.X.; investigation, X.X.; resources, X.X.; data curation, X.X.; writing—original draft preparation, X.X.; writing—review and editing, X.X.; visualization, X.X.; supervision, X.X.; project administration, X.X.; funding acquisition, Y.Y. All authors have read and agreed to the published version of the manuscript.”, please turn to the [CRediT taxonomy](#) for the term explanation. Authorship must be limited to those who have contributed substantially to the work reported.

**Funding:** Please add: “This research received no external funding” or “This research was funded by NAME OF FUNDER grant number XXX.” and “The APC was funded by XXX”. Check carefully that the details given are accurate and use the standard spelling of funding agency names at <https://search.crossref.org/funding>, any errors may affect your future funding.

**Data Availability Statement:** In this section, please provide details regarding where data supporting reported results can be found, including links to publicly archived datasets analyzed or generated during the study. Please refer to suggested Data Availability Statements in section “MDPI Research Data Policies” at <https://www.mdpi.com/ethics>. You might choose to exclude this statement if the study did not report any data.

**Acknowledgments:** In this section you can acknowledge any support given which is not covered by the author contribution or funding sections. This may include administrative and technical support, or donations in kind (e.g., materials used for experiments).

**Conflicts of Interest:** Declare conflicts of interest or state “The authors declare no conflict of interest.” Authors must identify and declare any personal circumstances or interest that may be perceived as inappropriately influencing the representation or interpretation of reported research results. Any role of the funders in the design of the study; in the collection, analyses or interpretation of data; in the writing of the manuscript, or in the decision to publish the results must be declared in this section. If there is no role, please state “The funders had no role in the design of the study; in the collection, analyses, or interpretation of data; in the writing of the manuscript, or in the decision to publish the results”.

### Nomenclature

The following abbreviations and variables are used in this manuscript:

## Abbreviations:

A	Alternator
CSP	Concentrating solar power
EES	Engineering Equation Solver
HTR	High temperature recuperator
HX	Heat exchanger
LFR	Lead-fast reactor
LTR	Low temperature recuperator
MC	Main compressor
NREL	National Renewable Energy Laboratory
P	Pump
PC	Pre-cooler
RC	Re-compressor
sCO <sub>2</sub>	Supercritical carbon dioxide
T	Turbine
TES	Thermal energy storage

## Variables [Units]:

CR	Capacitance Ratio [-]
$\dot{C}$	Capacitance Rate [W/K]
$\Delta$	Temperature difference [K]
$\delta$	Approach temperature of heat exchanger [K]
$\varepsilon$	Effectiveness of heat exchanger [-]
$\eta$	Isentropic efficiency [-]
$h$	Enthalpy [J/kg]
$\dot{m}$	Mass flow rate [kg/s]
NTU	Number of transfer units [-]
$P$	Pressure [Pa]
$\dot{Q}$	Heat transfer rate [W]
$T$	Temperature [K]
UA	Conductivity of heat exchanger [W/K]
$v$	Volumetric flow rate [ $m^3/kg$ ]
$\dot{W}$	Power [W]
$y$	Splitter Fraction [-]

```
#My ees file
def myfunc():
    return x
x = y

f = 8*y^2
```

$$a^2 + b^2 = c^2 \quad (5)$$

## References

1. Wagner, M.J. Optimization of stored energy dispatch for concentrating solar power systems. PhD thesis, Colorado School of Mines, 2017.
2. Blair, N.; Dobos, A.; Freeman, J.; Gilman, P.; Janzou, P.; Wagner, M.; Neises, T.; Mehos, M. SAM five year solar technologies roadmap. *Applied energy* **2005**, *231*, 1109–1121.
3. Hirsch, T.; Eck, M.; Blanco, M.J.; Wagner, M.; Feldhoff, J.F. Standardization of CSP Performance Model Projection: Latest Results From the guiSmo Project. *Energy Sustainability*, 2011, Vol. 54686, pp. 737–742.
4. Nellis, G.; Klein, S. *Heat Transfer*; Cambridge University Press, 2008. doi:10.1017/CBO9780511841606.